The Activity and Size of the Nucleus of Comet Hale-Bopp (C/1995 O1)

H. A. Weaver,* P. D. Feldman, M. F. A'Hearn, C. Arpigny, J. C. Brandt, M. C. Festou, M. Haken, J. B. McPhate, S. A. Stern, G. P. Tozzi

Analysis of Hubble Space Telescope (HST) images of comet Hale-Bopp (C/1995 O1) suggests that the effective diameter of the nucleus is between 27 to 42 kilometers, which is at least three times larger than that of comet P/Halley. The International Ultraviolet Explorer and HST spectra showed emissions from OH (a tracer of H_2O) and CS (a tracer of CS_2) starting in April 1996, and from the CO Cameron system (which primarily traces CO_2) starting in June 1996. The variation of the H_2O production rate with heliocentric distance was consistent with sublimation of an icy body near its subsolar point. The heliocentric variation in the production rates of CS_2 and dust was different from that of H_2O, which implies that H_2O sublimation did not control the CS_2 or dust production during these observations.

Comet Hale-Bopp (C/1995 O1) is an exceptionally active comet that was discovered in July 1995 (*1*) at a heliocentric distance (r_h) of 7.2 astronomical units (AU; 1 AU = 1.495×10^{11} m is the average Earth-sun distance). At r_h = 6.5 AU the comet was already producing CO at the rate of $\sim 10^3$ kg s^{-1} (*2, 3*), which is comparable to that produced from the nucleus of comet Halley near r_h = 1 AU. Because the activity in long-period comets, like Hale-Bopp, usually scales as r_h^{-2}, or even faster, spectroscopic observations of Hale-Bopp are possible over a large range in r_h as the comet moves toward perihelion on 1 April 1997, when r_h = 0.91 AU. Of particular interest is how the rate of ice sublimation changes with increasing solar insolation, including variations among the different ices present in the nucleus, and the relationship between the subliming ices and the dust particles that are dragged away from the nucleus, creating the visible coma. In addition, imaging and spectroscopic observations of short-term temporal variations of Hale-Bopp can be used to probe physical and chemical characteristics of the nucleus that might trigger outbursts in activity, such as amorphous to crystalline phase changes in H_2O ice, chemical inhomogeneity in the ices, and the unmantling of vents on the surface that were previously covered by refractory debris.

The pre-perihelion activity of Hale-Bopp was monitored with the International Ultraviolet Explorer (IUE) from August 1995 until IUE was decommissioned in September 1996 and with HST until the comet reached the solar elongation limit of HST in October 1996 (Table 1). Images were taken with the Wide Field Planetary Camera 2 (WFPC2) (*4*) to estimate the size of the nucleus and to study its activity. Emissions from molecules and dust in the coma were studied using the Faint Object Spectrograph (FOS) of HST (*5*) and the Long-Wave Prime spectrograph of IUE.

Size of the nucleus. Because the width of a WFPC2 pixel projected to 90 km at the comet for the minimum geocentric distance (Δ) of the HST observations (2.74 AU), which is much larger than a typical comet, we did not expect to resolve the smaller nucleus. However, when the coma does not have complex spatial structure and its spatial brightness profile can be described by a simple analytic function, the effective scattering cross section of the nucleus can be estimated if extrapolation of the coma into the unresolved region fails to account for the observed intensity of the peak pixel. We can calculate the effective diameter of the nucleus from a standard formula (*6*). This method has been applied for observations of two active comets having $\Delta \sim 0.6$ AU (*7, 8*). Extending the method to active comets at larger Δ is problematic because the required extrapolation of the coma increases linearly with increasing Δ.

For uniform, spherically-symmetric outflow of dust from the nucleus, the nucleus to coma contrast ratio should be inversely proportional to Δ (*9*) and the dust production rate (Q_{dust}). While this suggests that the nucleus should be most easily detected in the June and July 1996 images (Fig. 1), temporal variability caused deviations in the spatial brightness profiles for these images that precluded making an unambiguous extrapolation of the coma into the unresolved region. We concluded that the October 1995 image (Fig. 1) was best for determining the size of the nucleus, primarily because relatively quiescent conditions prevailed.

Spatial brightness profiles for the October 1995 data can be described by power laws (Fig. 2). The power law exponents derived for the profiles (−0.94 along a faint radial jet and −1.16 in the opposite direc-

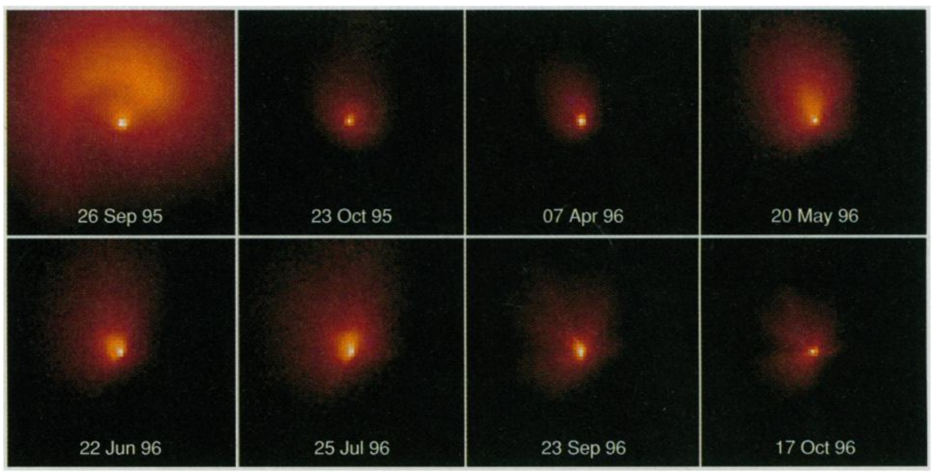

Fig. 1. HST images of Hale-Bopp interpolated to the same spatial scale of 470 km per pixel (each image covers a distance of ~33,000 km at the comet), normalized to the same peak pixel intensity, and displayed using the same logarithmic intensity scale. In all images, celestial north is straight up (vertical direction) and east is to the left. The image from 7 April 1996 was slightly trailed due to poor tracking.

H. A. Weaver, P. D. Feldman, J. B. McPhate, Department of Physics and Astronomy, Johns Hopkins University, Baltimore, MD 21218, USA.
M. F. A'Hearn and M. Haken, Department of Astronomy, University of Maryland, College Park, MD 20742, USA.
C. Arpigny, Institut d'Astrophysique, Université de Liège, B-4000 Liège, Belgium.
J. C. Brandt, Laboratory for Atmospheric and Space Physics, University of Colorado, Boulder, CO 80309, USA.
M. C. Festou, Observatoire Midi-Pyrénées, 14 avenue E. Belin, F-31400, Toulouse, France.
S. A. Stern, Southwest Research Institute, Space Science Department, Boulder Extension Office, 1050 Walnut Drive, Suite 426, Boulder, CO 80302, USA.
G. P. Tozzi, Osservatorio Astrofisico di Arcetri, Largo E. Fermi 5, I-50125, Florence, Italy.

*To whom correspondence should be addressed.

Table 1. Log of HST and IUE Hale-Bopp observations. WFC and PC refer to the wide-field and planetary modes, respectively, of WFPC2. Distances, r_h and Δ are given in astronomical units. $\dot{r}_h$ is the heliocentric radial velocity of the comet in kilometers per second. ϕ is the phase angle (sun-comet-Earth angle) in degrees. B is the observed column brightness in rayleighs averaged over the spectrograph aperture (1 rayleigh = 10^6 photons cm^{-2} s^{-1}) for the OH (0,0) band near 3090 Å, the CS $\Delta v = 0$ band sequence near 2576 Å, and the CO (1,0) Cameron band near 1995 Å. We used a rectangular FOS aperture whose size was 3.66 arc sec by 1.29 arc sec, except that a circular aperture of diameter 0.86 arc sec was used for some observations on 18 October 1996. The FOS aperture was usually nearly centered on the nucleus, but the aperture was offset ~5-6 arc sec east and ~0.5 arc sec east for the April 1996 and October 1996 FOS observations, respectively. The IUE observations were made with a rectangular aperture (9.3 arc sec by 15 arc sec) that was centered on the nucleus. Q is the calculated production rate at the surface of the nucleus. For the gaseous molecular species, Q is given in molecules per second, while Q_{dust} is given in $r\sigma^{-3}$ kg s^{-1}. $Af\rho$ is an aperture-independent measure of the dust production in meters, as defined in the text. Dual values are given for some of the September 1996 entries, and these refer to pre- and post-outburst measurements. The quoted errors are 1σ values, except that 3σ values are quoted for entries in which only upper limits are available.

Date	Instrument	r_h	Δ	$\dot{r}_h$	ϕ	B_{OH}	B_{CS}	B_{CO}	Q_{H_2O} (10^{28})	Q_{CS_2} (10^{26})	Q_{CO_2} (10^{28})	$Af\rho$	Q_{dust}
31 Aug. 1995	IUE	6.82	6.31	−14.9	7.6	—	—	—	—	—	—	1410	12.0
3–4 Sep. 1995	IUE	6.80	6.33	−14.9	7.9	—	—	—	—	—	—	1190	10.1
26–27 Sep. 1995	WFC	6.59	6.51	−15.1	8.7	—	—	—	—	—	—	1430	12.4
23–25 Oct. 1995	PC, FOS	6.36	6.72	−15.4	8.2	≤18	≤6.3	≤14	≤1.7	≤0.29	≤21	640	5.6
7 April 1996	PC, FOS	4.79	4.80	−17.2	12	35 ± 5	10 ± 2	—	2.0	1.2	—	1060	10.8
21 April 1996	IUE	4.65	4.42	−17.4	12	—	—	—	—	—	—	1410	14.5
13 May 1996	IUE	4.43	3.85	−17.7	11	60 ± 15	20 ± 5	—	2.5	1.0	—	1170	12.3
20 May 1996	PC	4.35	3.68	−17.9	11	—	—	—	—	—	—	1280	13.6
22–23 June 1996	PC, FOS	4.00	3.01	−18.4	4.4	345 ± 40	90 ± 14	13 ± 4	6.2	0.98	4.4	1050	11.7
25–26 July 1996	PC, FOS	3.65	2.74	−19.0	8.2	770 ± 70	140 ± 25	11 ± 4	10	1.2	3.0	1210	14.1
25 Aug. 1996	IUE	3.31	2.79	−19.6	16	1000 ± 100	110 ± 20	—	14	2.7	—	1520	18.5
23 Sep. 1996	PC, FOS	2.97	2.95	−20.2	19	3600 ± 200	390 ± 30	41 ± 6	21	2.2	8.8	2120	27.3
						4500 ± 800	830 ± 100		26	4.6		7290	93.9
17–18 Oct. 1996	PC, FOS	2.69	3.94	−20.8	19	7000 ± 700	740 ± 100	20 ± 5	27	3.0	3.4	1950	26.4

tion) are consistent with theoretical expectations and with the profiles observed in other comets (*10*). Although none of the HST images showed steady-state spherically symmetric outflow, the October 1995 image most closely approximates this condition. Extrapolation of the coma into the core of the image (the peak pixel) leaves a residual intensity that we attribute to scattered light from the nucleus (*11*). Assuming that the geometric albedo of the nucleus is 4%, which is the value observed for Halley (*12*), we estimate that the nucleus of Hale-Bopp has a diameter of at least 27 km and could be as large as 42 km (*13*). The amount of subliming ice near the subsolar point on the nucleus needed to explain the observed H_2O production rate is ~6% of the area of a 42-km nucleus and ~14% of the area of a 27-km nucleus. For comparison, the nucleus of comet Halley was 8 km × 8 km × 16 km, which corresponds to an effective spherical diameter of ~10 km, and ~10% of its total surface area was active (*12*). For a sample of 12 periodic comets having measured diameters, the estimated fractional area covered by subliming ice ranges from ≤0.5% to ~15% (*14*).

If there was a strong dust outburst shortly before our October 1995 observations, then the brightness cusp in the core that we are attributing to the nucleus could instead be due to newly created dust. The deviations of the observed coma spatial brightness profiles from that of a simple power law indicate that some low-level temporal variability was present during the October observations. However, ground-based monitoring of the inner coma of Hale-Bopp shows that the October 1995 HST observations were obtained when the coma brightness was decreasing with time following the large outburst that occurred near 13 October (*15*), consistent with the hypothesis that the excess core brightness was not caused by some transient event.

Gas and dust production rates. Ultraviolet (UV) gaseous emissions from Hale-Bopp were first detected during the April 1996 HST observations at r_h = 4.79 AU (*16*). The OH (0,0) band (in the $A^2\Sigma$-$X^2\Pi$ system) was observed near 3090 Å and the CS $\Delta v = 0$ band sequence (in the $A^1\Pi$-$X^1\Sigma$ system) was observed near 2576 Å. Starting in June 1996, two bands in the CO Cameron system ($a^3\Pi$-$X^1\Sigma$) became detectable (Fig. 3). We assumed that OH and CS were photolysis products of H_2O and CS_2, respectively, as is typically the case in other comets (*17*). The observed OH brightnesses were converted to aperture-averaged OH

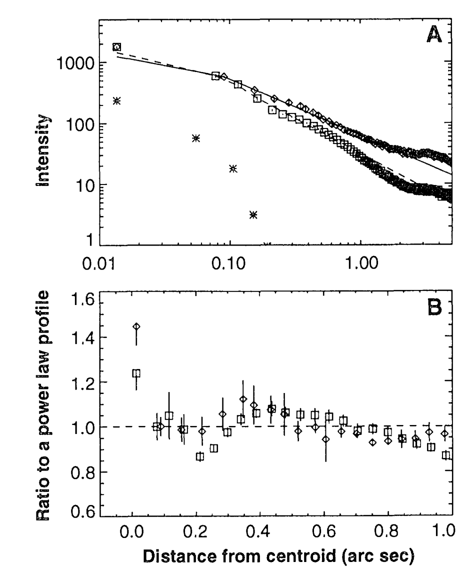

Fig. 2. Spatial brightness profiles (**A**) constructed from an HST image taken on 23 October 1995. One profile (diamonds) includes all data having an azimuthal extent of ±5° about the direction (~5° west of north) aligned with a weak, but persistent coma jet, while the other profile (squares) includes all data within a 90° wedge whose bisector is opposite the jet. The profiles can be fit by power laws having indices of −0.94 (solid line) and −1.16 (dashed line). The model power law profiles have been convolved with the WFPC2 point spread function (PSF), which causes the flattening at the shortest distances from the centroid. Extrapolation of these power laws into the core of the image yields brightnesses that are less than the observed brightness in the peak pixel, indicating that the nucleus has been photometrically resolved from the coma. The PSF (asterisks) has been scaled so that its intensity corresponds to that expected from a nucleus having a diameter of 27 km, assuming that the geometric albedo is 4%. The signature of the nucleus is seen more clearly in (**B**), where the observed profiles have been divided by the model power law profiles. The minimum value for the first data point (the nominal value minus the estimated statistical error) corresponds to an effective nucleus diameter of 27 km, while the maximum value implies a diameter of 42 km.

column densities assuming optically thin conditions and using "quenched" fluorescence efficiency factors, or g-factors (*18*). The OH column densities were then converted to H_2O production rates (Q_{H_2O}) at the nucleus using a spherically symmetric "vectorial" density model (*19*) (Table 1 and Fig. 4). Column densities for CS were calculated assuming that the CS emission was optically thin and using a g-factor of 7×10^{-4} photons s^{-1} molecule^{-1} (*20*). We then used a standard Haser formula (*21*) to calculate the CS_2 production rates (Q_{CS_2}) (Table 1 and Fig. 4).

For comparison with the observations, we computed the surface-averaged sublimation rate for a nucleus composed of H_2O ice under two conditions: (i) for an isothermal body and (ii) for a nucleus whose pole is pointing directly at the sun. We also calculated the sublimation rate for a flat icy surface at the subsolar point. In all cases we assumed that the surface has unit infrared emissivity and an optical Bond albedo of 4% (*22*). The observed variation of Q_{H_2O} with r_h does not follow the curve expected for an isothermal body but is consistent with either of the other two cases (Fig. 4). The data favor the icy flat surface case, but the value of Q_{H_2O} on 7 April 1996 is probably at least partially due to the sublimation of icy grains in the coma, which means that our derived production rate is larger than the sublimation rate at the nucleus (*23*). The derived heliocentric variation in Q_{H_2O} does not depend on our model assumptions, but the absolute values are model-dependent. If we use "unquenched" OH g-factors, then Q_{H_2O} increases by a factor of ~1.5. If we use a hydrodynamic model for the OH density distribution, in which H_2O and OH have the same outflow velocity, then Q_{H_2O} decreases by a factor of ~0.7. Radio observations of OH emission in Hale-Bopp (*24*) yielded estimates of Q_{H_2O} similar to ours when all data were analyzed using consistent model parameters.

The heliocentric variation in Q_{CS_2} is different from that of Q_{H_2O}, at least for the largest values of r_h. This implies that the release of CS_2 from the nucleus was not controlled by H_2O sublimation and that CS_2 molecules in the nucleus are not trapped within H_2O ice. Although H_2O is apparently the most abundant ice in cometary nuclei, the trace volatile constituents may not be as intimately mixed with the H_2O ice as is sometimes assumed.

Observations of CO Cameron band emission can be used to derive production rates for CO and CO_2 (*25*), but this technique is limited by our inability to specify the rate constants for the two important excitation mechanisms, photoelectron impact on CO and "prompt" emission following the photodissociation of CO_2. Given the larger uncertainty associated with photoelectron impact processes in comae, particulary at large r_h, we considered only the prompt process, which yields an upper limit to the CO_2 production rate (Q_{CO_2}) (Table 1) (*26*).

The Infrared Space Observatory (ISO) observed Hale-Bopp (*27*) and found a Q_{CO_2} of 1×10^{28} molecules s^{-1} and 5×10^{28} molecules s^{-1} on 27 April 1996 and 27 September 1996, respectively, similar to our estimates (Table 1), which is significant considering the fact that temporal variability in Hale-Bopp may cause variability in Q_{CO_2}. The agreement in the HST and ISO values of Q_{CO_2} suggests that photodissociation of CO_2 is the dominant excitation mechanism for the observed CO Cameron band emission in Hale-Bopp and that photoelectron impact plays a minor role. The poor signal to noise ratio for the Cameron emission prevents us from saying much about the heliocentric variation of Q_{CO_2}, except to conclude that Q_{CO_2} during the September 1996 HST observation was higher than that measured on the other three dates of HST observations.

From the HST images, the HST spectra, and the IUE spectra, we calculated *Afρ* (Table 1), the product of the dust albedo, the dust filling factor, and the radius of the effective circular aperture used during the observations (*28*). This quantity is directly proportional to the observed continuum flux and was defined to provide an aperture-independent measure of the dust production rate.

Given the large uncertainties in the

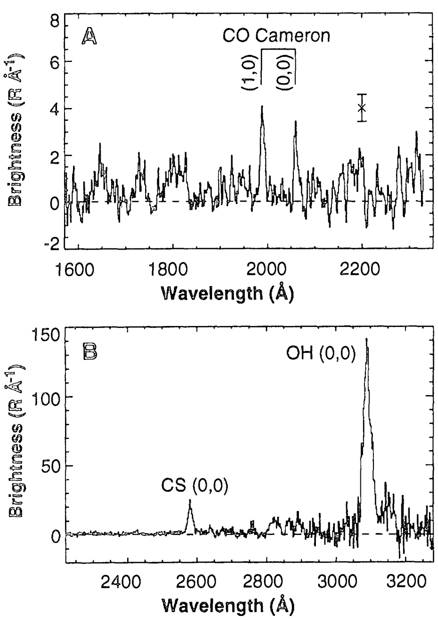

Fig. 3. The spectrum of Hale-Bopp taken on 23 September 1996. (**A**) The data for wavelengths shorter than 2220 Å were obtained from a 58-min exposure using the FOS G190H grating and the blue detector. (**B**) The longer wavelength data were from a 24-min exposure using the FOS G270H grating and the red detector. The continuum due to scattered sunlight from cometary dust has been subtracted from both sets of data. In addition, the pseudo-continuum produced by grating scattered light has also been removed from the G190H data. The dust continuum increases toward the longest wavelengths, which is why there is larger noise at the long wavelength end of (B). The error bar in (A) gives the $\pm 1\sigma$ statistical noise in the vicinity of the CO Cameron bands. The small excess signal near 1800 Å is probably due to emission in an atomic sulfur multiplet. The effective spectral resolution was ~4.5 Å and ~6 Å for the G190H and G270H data, respectively.

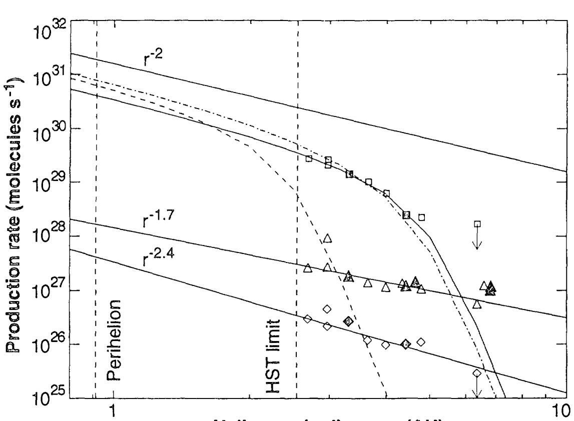

Fig. 4. Derived production rates for H_2O (squares), CS_2 (diamonds), and dust (triangles) (in kilograms per second multiplied by 1×10^{23}). The points with open symbols were derived from HST observations, while those with filled symbols were derived from IUE data. The points with the downward-pointing arrows are 3σ upper limits. The production rates of the three species have different heliocentric variations, indicating that no single physical mechanism controls their behavior. Water sublimation curves were computed for three different cases: the average rate over an isothermal spherical nucleus (dashed curve), the average rate over a spherical nucleus whose rotation axis is pointing directly at the sun (dot-dashed curve), and the local rate at the subsolar point (solid curve). The line labeled r_h^{-2} shows the heliocentric variation when sublimation dominates heating of the nucleus in the energy balance equation for any pure ice. The CS_2 and dust production rates can be fit with power law profiles having exponents of −2.4 and −1.7, respectively.

dust size distribution, density, albedo, and outflow speed, Q_{dust} derived here (*29*) (Table 1) may be different from the actual dust mass loss rate in Hale-Bopp. Our assumptions imply that $Q_{dust} = 22$ ($Af\rho$) for $r = 1$ AU, whereas an empirical relation derived from observations of a dozen comets near 1 AU (*31*) gives $Q_{dust} = 100$ ($Af\rho$). This discrepancy may be explained if the dust in Hale-Bopp moves more slowly than the dust in typical comets (for example, 0.5 km s^{-1} is usually quoted for comets at $r_h \sim 1$ AU whereas we assumed a velocity of 0.13 km s^{-1} for the dust in Hale-Bopp), but differences in the size, albedo, and density of the dust may also be important. The r_h dependence of Q_{dust} is different from that of Q_{H_2O}, which indicates that H_2O did not drive the dust activity in Hale-Bopp. CS_2 probably did not drive the dust activity either, since Q_{CS_2} (in kg s^{-1}) is ~1000 times smaller than Q_{dust}.

The weak dependence of Q_{dust} on r_h implies that Hale-Bopp will not be as bright during the spring of 1997 as originally expected. The brightness integrated over the entire coma for long-period comets like Hale-Bopp typically varies as r_h^{-6}, which translates into a r_h^{-4} variation in Q_{dust} (*32*). If our observed trend in Q_{dust} continues through perihelion, then the visual magnitude of Hale-Bopp will only reach ~0-1. The latter corresponds to a very bright comet but means that Hale-Bopp might be slightly fainter than comet Hyakutake (C/1996 B2) during its close approach to Earth last spring. If Q_{dust} becomes correlated with Q_{H_2O} as the comet nears perihelion, Hale-Bopp could be somewhat brighter than our predicted value (by a factor of ~2 or so; a change by one visual magnitude corresponds to a brightness change of a factor of 2.5). The comet could become brighter than our prediction if emission from the C_2 molecule increases rapidly near perihelion and becomes the major contributor (≳50%) to the visual magnitude.

Temporal variability. The 1995 ground-based observations showed that Hale-Bopp was periodically releasing large amounts of dust, apparently coinciding with the rotation of an active region on the nucleus into sunlight (*30*). Our HST image from September 1995 (Fig. 1) was taken ~60 hours after one such outburst and shows the spiral coma structure that resulted. Analysis of the spatial brightness profiles for this HST image indicates that Q_{dust} during the outburst exceeded the quiescent value by a factor of ~7. None of the other HST images displayed a coma morphology similar to that seen in the September 1995 outburst, but all of them displayed evidence of temporal variability. During the fall of 1996, multiple coma jets became visible, possibly signaling an increase in the activation rate of vents on the surface of the nucleus.

During our September 1996 spectroscopic observations, we serendipitously caught Hale-Bopp as it experienced a large outburst in dust and gas. The dust continuum, which had been steady at the 5% level for at least 3.5 hours, suddenly increased by a factor of 3.4 between two spectra that were separated by 77 min and continued increasing at ~1.2% min^{-1} for the final 8 min of our observations (*33*). The CS emission increased by a factor of 2.1 over this same period, while no change was observed in the OH emission. We could not find any noncometary explanations for the observed changes, so we conclude that the comet itself was varying over time (*34*).

Because our observations essentially average the production rates over the aperture-crossing time, the observed changes in the continuum and CS intensities only give lower limits to the actual changes in Q_{dust} and Q_{CS_2}. Using time-dependent models, we find that Q_{dust} during the outburst was at least a factor of 8 larger than the quiescent value (*35*) and that Q_{CS_2} increased by a factor of ~3 (*36*). The model also demonstrates that no change was expected in the OH emission, even if Q_{H_2O} changed because the H_2O lifetime is much longer than the duration of the observed changes. These temporal variations in Hale-Bopp indicate that the surface of the nucleus must be dynamic. Perhaps the temporal variation is associated with the activation of a new vent on the surface. It is also conceivable that the temporal changes were caused by compositional inhomogeneity in a previously active vent, but we have no observational confirmation of any compositional variation during the outburst.

REFERENCES AND NOTES

1. A. Hale and T. Bopp, *IAU Circular 6187* (1995).
2. D. Jewitt, M. Senay, H. Matthews, *Science* **271**, 1110 (1996).
3. N. Biver *et al.*, *Nature* **380**, 137 (1996).
4. The WFPC2 consists of three wide-field mode charged-coupled devices (CCDs) having 0.0996 arc sec $pixel^{-1}$ and one planetary mode CCD having 0.0455 arc sec per pixel. The point spread function (PSF) of the planetary mode has a full-width at half-maximum of ~0.070 arc sec, which projects to 250 km at a geocentric distance of 5 AU. Further information on the WFPC2 is available at http://www.stsci.edu/ftp/instrument_news/WFPC2/wfpc2_top.html
5. The FOS is a versatile instrument that can provide moderate and low resolution spectra over the wavelength range from 1140 Å to 9000 Å by employing multiple gratings and two one-dimensional digicon detectors coated with different photocathodes. During our observations, we used the G190H and G270H gratings, which together covered the wavelength range from 1570 Å to 3300 Å at a resolving power of ~1000 for the cometary emissions having a sharply-peaked spatial distribution. Further information on the FOS is available http://www.stsci.edu/ftp/instrument_news/FOS/topfos.html
6. H. A. Weaver *et al.*, *Science* **263**, 787 (1994). The WFPC2 CCD signal measured through the F675W filter and attributed to the nucleus can be converted to an R magnitude in the Landolt-Kron-Cousins photometric system using standard relations given in (*4*). Then the diameter of the nucleus, d_N (km), can be calculated using:

$$d_N = [(2.99 \times 10^8) \, 10^{0.2(m_{sun} - m_{comet}) + 5 \log(r\Delta) + 0.035 \phi}]/A_p{}^{0.5}$$

where m_{sun} (= −27.10) is the R magnitude of the sun, m_{comet} is the R magnitude of the nucleus, and A_p is the geometric albedo.
7. P. L. Lamy and I. Toth *Astron. Astrophys.* **293**, L43 (1995).
8. P. L. Lamy, I. Toth, H. A. Weaver, *Astron. Astrophys.*, in preparation.
9. L. V. Wallace and F. D. Miller, *Astron. J.* **63**, 213 (1958). The results from this report can be used to demonstrate that the coma flux observed in a circular aperture of fixed angular dimensions scales as Δ^{-1}. The flux from the nucleus is independent of aperture size and scales as Δ^{-2}.
10. D. C. Jewitt, in *Comets in the Post-Halley Era*, R. L. Newburn, M. Neugebauer, J. Rahe, Eds. (Kluwer, Dordrecht, 1991).
11. All of our non-trailed HST images taken in planetary mode show a brightness cusp at the peak pixel that we interpret as the signature of the nucleus. However, if icy grains dominated the dust population within a few hundred kilometers of the nucleus and evaporated into lower albedo particles outside this region, then the brightness cusp could be due to coma rather than the nucleus. On the other hand, a continuous degradation of dust albedo with cometocentric distance would steepen the coma surface brightness profile, causing us to underestimate the size of the nucleus. Similarly, dust fragmentation in the coma could cause us to underestimate or overestimate the size of the nucleus, depending on the exact nature of the fragmentation.
12. H. U. Keller *et al.*, *Astron. Astrophys.* **187**, 807 (1987).
13. While the signal-to-noise ratio in the peak pixel is large (over 100), the error in estimating the size of the nucleus is determined by systematic effects. In particular, the derived size depends on the extrapolation of the coma into the unresolved region. Light scattered from a 42-km nucleus only contributes ~37% of the brightness in the peak pixel, so the coma dominates the observed light distribution even in the core of the image. The nucleus has to be large in order to detect its signature in the presence of such a bright coma, and a Halley-sized object would be undetectable with HST.
14. M. F. A'Hearn *et al.*, *Icarus* **118**, 223 (1995).
15. M. R. Kidger *et al.*, *Astrophys. J. Lett.*, in preparation.
16. H. A. Weaver, *IAU Circular 6376* (1996).
17. ______, P. D. Feldman, M. C. Festou, M. F. A'Hearn, H. U. Keller, *Icarus* **47**, 449 (1981).
18. D. G. Schleicher and M. F. A'Hearn, *Astrophys. J.* **331**, 1058 (1988); F. P. Schloerb, *Astrophys. J.* **332**, 524 (1988). "Quenched" means that the populations of the two Λ-doubled components of the lowest rotational level are equally populated due to collisions.
19. M. C. Festou, *Astron. Astrophys.* **96**, 69 (1981); S. A. Budzien, M. C. Festou, P. D. Feldman, *Icarus* **107**, 164 (1994). We assumed that the H_2O outflow velocity was 0.8 $r_h^{-0.5}$ km s^{-1} (for the IUE observations we used 0.85 $r_h^{-0.5}$ km s^{-1}; photolytic heating of the coma causes the average outflow velocity to increase with increasing distance from the nucleus, so the average velocity is larger in the larger IUE aperture), the total H_2O lifetime was $8.2 \times 10^4 \, r_h^2$ s, 84% of the H_2O destruction produced OH, the OH was ejected isotropically in the frame of the dissociating H_2O molecule with a velocity of 1.05 km s^{-1}, and that the OH lifetime was $1.6 \times 10^5 \, r_h^2$ s.

20. W. M. Jackson, J. B. Halpern, P. D. Feldman, J. Rahe, *Astron. Astrophys.* **107**, 385 (1982).
21. L. Haser, *Bull. Acad. R. Sci. Liège* **43**, 740 (1957). The CS_2 lifetime (500 r_h^2 s) is so short that we assume that collisions equilibrate the CS_2 and CS velocities to the same value (0.8 $r_h^{-0.5}$ km s^{-1} and 0.85 $r_h^{-0.5}$ km s^{-1} for the HST and IUE data, respectively). Examination of the relevant collision rates indicates that this assumption is justified for most of the 1996 observations but may not be valid at the larger values of r_h. Using a vectorial model raises Q_{CS_2} by a factor of ~2 relative to the Haser model result at all values of r_h. Thus, using a single model, either Haser or vectorial, does not change the power law index for the r_h variation of Q_{CS_2}. Using a vectorial model at large r_h and a Haser model at small r_h would produce a smaller power law index, which strengthens our conclusion that Q_{CS_2} and Q_{H_2O} had different variations with r_h. We assumed that a CS molecule is produced for every CS_2 molecule that is destroyed, and we used a CS lifetime of $1 \times 10^5 r_h^2$ s.
22. J. J. Cowan and M. F. A'Hearn, *Moon and Planets* **21**, 155 (1979).
23. At large r_h the activity in Hale-Bopp was apparently driven by the sublimation of CO ice (*2, 3*), which means that dust grains in the coma may have retained a H_2O ice mantle. Owing to their low efficiency at radiating heat, micrometer-sized grains can become warmer than the nucleus, which means that H_2O in the coma at large r_h could be due primarily to sublimation from these icy grains and that our values of Q_{H_2O} no longer refer to H_2O production from the nucleus. As is typically the case for comets, H_2O sublimation from the nucleus of Hale-Bopp presumably became the dominant source of H_2O in the coma at some point. Perhaps the best evidence for the latter is the agreement between our model sublimation curves and the observed values of Q_{H_2O}. The activation of several new vents on the surface of the nucleus during mid-1996, as observed in ground-based images of Hale-Bopp, may also have signaled the transition from a CO-dominated comet to a H_2O-dominated one.
24. J. Crovisier *et al.*, paper on the radio observations of Hale-Bopp presented at the 28th Annual Meeting of the Division of Planetary Sciences of the American Astronomical Society, Tucson, AZ, 22 to 26 October 1996.
25. H. A. Weaver *et al.*, *Astrophys. J.* **422**, 374 (1994).
26. Assuming that CO_2 is flowing outward from the nucleus, the production rate is given by: $Q_{CO_2} = (7.25 \times 10^{18}) v \theta r_h^2 \Delta B / g$ where g is the rate constant, $v = 0.8\ r_h^{-0.5}$ km s^{-1}, B is the observed brightness of the Cameron (1, 0) band in rayleighs, and θ is the diameter of the equivalent circular aperture of 2.4 arc sec.
27. J. Crovisier *et al.*, *Science* **275**, 1904 (1997). We recomputed Q_{CO_2} derived from the ISO observations using an outflow velocity of 0.8 $r_h^{-0.5}$ in order to be consistent with the assumptions made in analyzing the HST data.
28. M. F. A'Hearn, D. G. Schleicher, P. D. Feldman, R. L. Millis, D. T. Thompson, *Astron. J.* **89**, 579 (1984). From the HST images, we calculated $Af\rho$ using a synthetic aperture having a diameter of 2 arc sec, which is close to the effective diameter of our most commonly used FOS aperture (2.4 arc sec). We found that $Af\rho$ varied with aperture size, typically at the 10 to 30% level, probably due to temporal variability in the comet. By comparing the HST imaging and spectral data, we found empirically that $Af\rho$ near 7000 Å, the effective wavelength of the F675W filter used for the WFPC2 observations, was ~1.9 times larger than $Af\rho$ near 2950 Å. Thus, we multiplied the raw IUE $Af\rho$ values near 2950 Å by 1.9 to convert them to their equivalent "optical" values. The $Af\rho$ values were converted to a common phase angle (the sun-comet-Earth angle), ϕ, of 0° by multiplying the raw values by $10^{(0.4)(0.035)\phi}$. A different choice for the phase law is unlikely to affect our conclusions, as Hale-Bopp was observed over a narrow range in phase angle.
29. For dust having an average radius a (in micrometers), density d (in grams per cubic centimeter), geometric albedo A_p, and flowing outward from the nucleus with velocity v_{dust} (in kilometers per second), the dust mass production rate, Q_{dust} (in kilograms per second) is given by: $Q_{dust} = (0.67) a d v_{dust} Af\rho / A_p$ where $Af\rho$ is in meters. We calculated Q_{dust} using $v_{dust} = 0.13\ r_h^{-0.5}$ (*30*), $a = 10$, $d = 1$, and $A_p = 0.04$ (Table 1 and Fig. 4).
30. Z. Sekanina, *Astron. Astrophys.* **314**, 957 (1996). From a detailed analysis of the dust coma, this author derived a dust ouflow velocity (v_{dust}) of ~0.05 km s^{-1} at r_h = 6.82 AU, and we have additionally assumed that $v_{dust} = 0.05\ (r_h/6.82)^{-0.5}$.
31. C. Arpigny *et al.*, *Atlas of Cometary Spectra* (Kluwer, Dordrecht, 1997).
32. L. Kamél, *Icarus* **122**, 428 (1996) and (*14*).
33. A spectrum ending at 14:05 universal time (UT) on 23 September 1996 had essentially the same continuum flux as other spectra that were taken between 10:30 and 14:05 UT. (The spectra were not continuously recorded during this latter period because the HST periodically passes behind the Earth, at which times the comet was not visible from HST. The HST orbital period is 96 min, and observations are generally limited to a duration of ~30 min each orbit.) Following a gap in our coverage due to Earth occultation, a 2-min spectrum starting at 13:41 UT had a continuum level that was 3.4 times larger than that recorded during the earlier times. In addition, three subsequent 2-min spectra showed the continuum intensity monotonically increasing at the rate of ~1.2% min^{-1}.
34. We ruled out pointing error as the source of the observed temporal variation by verifying that the flux measured in spectra taken immediately before the outburst was essentially identical to that measured during observations spanning up to ~6.5 hours earlier. A solar-type star entering the aperture and having a visual magnitude of ~11.5 could have produced the observed increase in the continuum, but no such object was present in the cometary field. Furthermore, another object entering the aperture would not explain the observed increase in CS emission. During the outburst, the spatial distribution of the continuum became markedly more peaked towards the nucleus, which is consistent with a dust outburst originating at the nucleus of the comet.
35. For spherically symmetric outflow of dust from the nucleus with velocity v, it is easy to show that the total number of grains, n_q, in a circular aperture of radius ρ is given by $n_q = (\pi/2)\ Q_q\ \rho/v$, where Q_q is the dust production rate (in particles per second) under steady-state conditions. The number of extra dust grains, n_o, created during an outburst of duration t is given by $n_o = Q_o\ t$, where Q_o is the extra production rate above the quiescent value averaged over the duration of the outburst. Since $n_o/n_q = 2.4$, ρ = 2570 km, and t = 4635 s for our observations, the ratio of these two production rates is given by $2.1/v$ when v is in kilometers per second. Using our adopted value for v (0.076 km s^{-1}) yields a Q ratio of 28. In cometary work it is usually assumed that the dust velocity is given by $v \sim 0.5\ r_h^{-0.5}$ [N. T. Bobrovnikov, *Astron. J.* **59**, 357 (1954)], which gives a Q ratio of 7 and implies that the total dust production rate averaged over the outburst was eight times the quiescent value.
36. Assuming that all of the molecules produced during the outburst are contained in the observing aperture, the number of daughter molecules, n_d, at time t following the outburst is related to the number of parent molecules, n_p, produced during the outburst by $n_d = n_p\ (1 - e^{-t/\tau})$, where τ is the parent lifetime. Using our adopted lifetimes for CS_2 and H_2O, and an outburst duration of 4635 s, we see that the increase in the number of CS molecules should be ~64% of the increase in the number of CS_2 molecules, while the number of extra OH molecules should increase by less than 1% of the increase in H_2O molecules.
37. Support for this work was provided by NASA through grant numbers GO-05844 and GO-06663 from the Space Telescope Science Institute (STScI), which is operated by the Association of Universities for Research in Astronomy, Inc., under NASA contract NAS5-26555. C. Arpigny gratefully acknowledges financial support by the Belgian Fonds National de la Recherche Scientifique. We thank A. Lubenow and A. Storrs of the STScI for expertly planning the HST observations of Hale-Bopp. We also express our gratitude to W. Wamsteker and H. Andernach for their strong support of the IUE Hale-Bopp program.

28 January 1997; accepted 3 March 1997

The Spectrum of Comet Hale-Bopp (C/1995 O1) Observed with the Infrared Space Observatory at 2.9 Astronomical Units from the Sun

Jacques Crovisier,* Kieron Leech, Dominique Bockelée-Morvan, Timothy Y. Brooke, Martha S. Hanner, Bruno Altieri, H. Uwe Keller, Emmanuel Lellouch

Comet Hale-Bopp (C/1995 O1) was observed at wavelengths from 2.4 to 195 micrometers with the Infrared Space Observatory when the comet was about 2.9 astronomical units (AU) from the sun. The main observed volatiles that sublimated from the nucleus ices were water, carbon monoxide, and carbon dioxide in a ratio (by number) of 10:6:2. These species are also the main observed constituents of ices in dense interstellar molecular clouds; this observation strengthens the links between cometary and interstellar material. Several broad emission features observed in the 7- to 45-micrometer region suggest the presence of silicates, particularly magnesium-rich crystalline olivine. These features are similar to those observed in the dust envelopes of Vega-type stars.

The infrared (IR) wavelength region is useful for investigating comets because (i) comets are cold and the thermal emission of the nucleus and dusty atmosphere peaks at IR wavelengths and (ii) the volatile molecular species, sublimated from cometary nucleus ices, can be identified through their fundamental bands of vibration, which are seen in fluorescence excited by solar radiation. IR observations of comets (*1–3*) from the ground are limited to a few atmospheric windows. IR spectra of comets above Earth's atmosphere